Identification of cold-stress responsive proteins in *Anabasis aphylla* seedlings via the iTRAQ proteomics technique

Tingting Wang, Chunxiu Ye, Mei Wang & Guangming Chu

Taylor & Francis
Taylor & Francis Group

RESEARCH ARTICLE

OPEN ACCESS

Check for updates

Identification of cold-stress responsive proteins in *Anabasis aphylla* seedlings via the iTRAQ proteomics technique

Tingting Wang[a], Chunxiu Ye[b,c], Mei Wang[a] and Guangming Chu[a]

[a]Agricultural College, Shihezi University, Shihezi, Xinjiang, People's Republic of China; [b]Xinjiang Agricultural University, Urumqi, Xinjiang, People's Republic of China; [c]Key Laboratory of Crop Germplasm Enhancement and Gene Resources Utilization, Xinjiang Production & Construction Group, Center for Molecular Agrobiotechnology and Breeding, Xinjiang Academy of Agricultural and Reclamation Sciences, Shihezi, Xinjiang, People's Republic of China

ABSTRACT

Cold stress is one of the major environmental factors that affects plant growth, development, and species distributions. In order to study the molecular mechanism of cold-stress responses in *Anabasis aphylla* seedlings, we used the isobaric tags for relative and absolute quantification (iTRAQ) technique to identify differential protein expression under cold stress. In total, 211 differentially expressed proteins were identified, including 109 up-accumulated proteins and 102 down-accumulated proteins, these cold-stress response proteins were mainly identified as proteins involved in carbohydrate and energy metabolism, protein metabolism and translation, stress response, transcription-related, amino acid metabolism, signal transduction, and membrane and transport. GO and Kyoto Encyclopedia of Genes and Genomes pathway enrichment analyses indicated that most of the proteins related to cold-stress response were involved in carbohydrate and energy metabolism, indicating *A. aphylla* seedlings adapted to cold conditions mainly through changes in energy metabolism pathways. Additionally, the correspondence between mRNA transcript levels and protein abundance levels for nine accumulated proteins were also tested by qRT-PCR, only one protein did not show consistent trends in mRNA and protein levels. These data clarify our current understandings of stress responses in seedlings of species such as *A. aphylla* and identify the molecular mechanisms of the cold-stress responses.

Introduction

Cold stress is a major abiotic factor that has noticeable effects on plant physiology and growth. It limits the geographical distribution and productivity of many wild plants and crops. Cold stress broadly influences the physiological and biochemical processes of plants, including photosynthesis (Hu et al. 2000), respiration (Xu 2007), oxygen and antioxidant enzymatic activity (Kang 2008), and water circulation (Sun 2011). In order to tolerate and adapt to adverse growth conditions, plants improve their cold resistance through the regulation of metabolic pathways. Plant responses to cold stress usually occur through changes in membrane composition, antioxidant components, and gene transcription rates under cold stress (Lukatkin 2002). Many genes that respond to cold stress have been documented in the model species *Arabidopsis thaliana* (Nordin et al. 1993; Welin et al. 1995; Medina et al. 1999). In recent years, proteomics combined with cold-resistant mutation analysis has significantly increased our understanding of signaling pathways and other important molecular mechanisms involved in cold acclimation (Chen et al. 2014; Janda et al. 2014). To date, proteomics has been used to analyze the cold resistance of a diverse array of plant species, including *Chorispora bungeana*, *Oryza sativa* (rice), *Musa nana* (dwarf banana), *Buchloe dactyloides*, and the desert woody plants *Ammopiptanthus mongolicus* and *Populus euphratica* (Yue et al. 2009; Tan 2012; Zhou 2013; Chen 2015; Pang 2015; Zhou et al. 2016), through this body of research, many proteins associated with cold-stress responses have been identified.

The subshrub *Anabasis aphylla* belongs to the family Chenopodiaceae and is one of the main species found in the soil desert area of the Junggar Basin, where it has an important role in water and soil conservation throughout the diluvial fan and plain. Furthermore, it is a plant species with great value (Wang et al. 2015). In this area, snowmelt is a vital water source for *A. aphylla* seed germination, and it can regulate plant phenology and ecosystem nutrient cycling. Through a combination of field investigation and observations with a simulation experiment, we found that a large number of *A. aphylla* seeds germinated in snowmelt in the field, which is consistent with *Anabasis elatior* germination characteristics (Han et al. 2011). Shimono and Kudo (2005) also found *Peucedanum multivittatum* seeds can germinate at 0°C and observed seeds that were buried in snow beds can emerge in the midst of freezing–thawing cycles. Thus, *A. aphylla* seeds clearly have the ability to germinate during snowmelt periods, and seedlings must therefore physiologically adapt to freezing conditions. This property has notable ecological significance for *A. aphylla* seeds and seedlings in coping with climatic fluctuations and unusually rapid warming in early spring.

Isobaric tags for relative and absolute quantification (iTRAQ) is a quantitative technique for analyzing cell metabolic changes. Many reports have used iTRAQ technology to identify and quantitatively analyze proteins. For example, Xie et al. (2016) successfully analyzed protein expression in tobacco leaves under drought stress. Wang (2013) identified differentially expressed proteins (DEPs) in *Lycium ruthenicum*

through the iTRAQ technique and subjected them to gene ontology (GO) analysis, which revealed significant overrepresentations of DEPs among some biological functions. Additionally, Wang et al. (2016) applied the quantitative analysis of DEPs in maize leaves under cold stress using the iTRAQ technique. However, there have been no published reports focused on cold adaptation in *A. aphylla*, which highlights the need for research on not only the cold resistance of *A. aphylla*, but also the expression of genes and proteins that respond to cold stress. This study therefore used the quantitative protein technology iTRAQ to identify and characterize the molecular mechanism of cold-stress responses in *A. aphylla* seedlings.

Materials and methods

Plant materials and stress treatments

A. aphylla seeds were obtained from the southern edge of the Gurbantünggüt Desert in Xinjiang, China. All collected *A. aphylla* seeds were sterilized by soaking them in 10% H_2O_2 for 30 min, after which they were rinsed with distilled water. For the control treatment, the sterilized seeds were germinated on filter paper discs soaked with distilled water in Petri dishes at room temperature and a 16-h light/8-h dark photoperiod until seedlings were approximately 3 cm in length. For the cold treatment, 3-cm-long seedlings were kept in a −3°C growth chamber for 12 h each day for 1 week. For each treatment, 3-g seedlings were selected as samples and quickly frozen in liquid nitrogen individually and stored at −80°C for protein extraction for iTRAQ-based comparative proteomic analyses. Both treatments had two biological replicates.

Protein extraction

Protein extraction was conducted according to the procedure described by Isaacson et al. (2006) with some modifications. Each *A. aphylla* sample was individually grinded into powder with liquid nitrogen. Then, 10 mL of cooled acetone containing 10% tricarboxylic acid (TCA) was added to 1 g of sample powder at −20°C for a 1-h incubation. Samples were then centrifuged at $15,000 \times g$ for 15 min at 4°C. The resulting pellet was collected, cooled acetone was again added at −20°C for another 1-h incubation, and the centrifugation and cooled acetone addition steps were then repeated again. After centrifugation at $15,000 \times g$ for 15 min at 4°C again, the resulting pellet was collected, dried with a vacuum freeze dryer, and suspended in cold phenol extraction buffer, to which an equal volume of phenol saturated with Tris–HCl (pH 7.5) was added. The mixture was maintained at 4°C for 30 min and then centrifuged at $5000 \times g$ for 30 min, after which the upper phenolic phase was collected and an equal volume of phenol extraction buffer was added. Thereafter, five volumes of cold 0.1 M ammonium acetate in methanol was added to the collected phenol phase, and the mixture was store at −20°C for a 1-h incubation and then centrifuged for 30 min at $5000 \times g$ at 4°C. Then two volumes (based on the volume of the last collected phenolic phase) of ice-cold methanol were used to wash the pellet, which was then mixed gently and centrifuged for 30 min at $5000 \times g$ at 4°C; this step was then repeated two more

times using acetone instead of methanol, and the sample was centrifuged for 30 min at $5000 \times g$ at 4°C. The pellet was then dried, dissolved in lysis solution at 30°C for a 1-h incubation, and centrifuged at $15,000 \times g$ for 15 min at room temperature. The supernatant was collected and centrifuged again. The resulting supernatant was the extracted protein solution. The concentrations of the protein extracts were determined using the bicinchoninic acid (BCA) method (Smith et al. 1985) and stored at −80°C before the subsequent iTRAQ analysis was conducted.

SDS-PAGE electrophoresis

For each replicate and treatment, 10-µg samples were subjected to electrophoresis in a 12% SDS-PAGE gel. The gel was visualized using Coomassie brilliant blue (CBB) stain according to Candiano's protocol (Giovanni et al. 2004). The gels were fixed for 2 h, stained for 12 h, and washed prior to the spots of interest being excised. The stained gel was scanned using an Image Scanner (GE Healthcare, USA) at a resolution of 300 dots per inch.

Protein reduction, cysteine blocks, and digests

For each spot of interest identified by SDS-PAGE, five volumes of cold acetone were added to 100 µg of each protein sample, incubated at −20°C for 1 h, and centrifuged at 12,000 rpm for 15 min at 4°C, and the resulting pellet was collected and dried with a vacuum freeze dryer. To each pellet, 50 µL of dissolution buffer and 4 µL of reducing reagent were added. The solution was incubated at 60°C for 1 h, and 2 µL of cysteine-blocking reagents was added, followed by a 10-min incubation at room temperature. The protein solution was then cleaned using a 10 kDa ultrafiltration tube by centrifugation at 12,000 rpm for 20 min, and then 100 µL of dissolution buffer was added, followed by centrifugation at 12,000 rpm for 15 min; this step consisting of adding dissolution buffer and centrifugation was repeated three times. The column was then placed in a new tube, to which 50 µL of sequencing-grade trypsin (50 ng/µL) was added, and incubated at 37°C for 12 h. The samples were then centrifuged at 12,000 rpm for 20 min, and the peptide was collected. The filter columns were then transferred to new collection tubes and 50 µL of dissolution buffer was added, after which the two filter solutions were combined.

Protein labeling and MS analysis

Each vial of iTRAQ reagent was brought to room temperature, with centrifugal iTRAQ reagent at the bottom of each reagent tube. Then, 150 µL of ethanol was added to each room-temperature iTRAQ reagent vial, and 50 µL of each sample (containing 100 µg of peptide) was added to new individual tubes, to which iTRAQ reagent was added, followed by incubation at room temperature for 2 h, after which 100 µL of water was added to halt the labeling reaction. The cold-treated sample replicates were labeled with iTRAQ tags 115 and 116, while the untreated samples were labeled with tags 113 and 114. After labeling, the samples were mixed and centrifuged, and the supernatant was collected. Finally, the sample was dried in a vacuum freeze dryer for iTRAQ analysis.

2D-LC-MS/MS analysis

Reverse-phase high-performance liquid chromatography

Dried samples were re-suspended with 100 μL of buffer A. Reverse-phase high-performance liquid chromatography (RPLC) was conducted on the Agilent 1200 HPLC System (Agilent, Santa Clara, CA, USA) using an Agilent HPLC column (narrow-bore 2.1 × 150 mm, 5 μm) with detection at 215 and 280 nm. Separation was performed at 0.3 mL/min. The first segment was collected between 0 and 5 min, and each subsequent segment was collected within 4.5 min intervals between 6 and 45 min, with the last segment collected between 46 and 50 min, yielding a total of 10 segments. Each segment was dried in a vacuum freeze dryer before LC-MS/MS analysis.

RPLC-MS/MS analysis

A. aphylla samples were re-suspended with Nano-RPLC buffer A. Online Nano-RPLC was conducted on the Eksigent nanoLC-Ultra™ 2D System (AB SCIEX, Framingham, MA, USA). The samples were loaded onto a C_{18} nanoLC trap column (100 μm × 3 cm, C_{18}, 3 μm, 150 Å) and washed with Nano-RPLC Buffer A (0.1% formic acid, 2% acetonitrile) at 2 μL/min for 10 min. An elution gradient of 5–35% acetonitrile (0.1% formic acid) over the course of a 70 min gradient was used on an analytical ChromXP C_{18} column (75 μm × 15 cm, C_{18}, 3 μm 120 Å) with a spray tip. Data acquisition was performed with a Triple TOF 5600 System (AB SCIEX) fitted with a Nanospray III source (AB SCIEX) and a pulled quartz tip as the emitter (New Objectives, Woburn, MA, USA). Data were acquired using an ion spray voltage of 2.5 kV, curtain gas at a pressure of 30 PSI, nebulizer gas at 5 PSI, and an interface heater temperature of 150°C. For information-dependent acquisition, survey scans were acquired in 250 ms, and as many as 35 product ion scans were collected if they exceeded a threshold of 150 counts per second with a 2^+ to 5^+ charge-state. The total cycle time was fixed at 2.5 s. A rolling collision energy setting was applied to all precursor ions for collision-induced dissociation. Dynamic exclusion was set for half of the peak width (18 s), and the precursor was then refreshed off the exclusion list.

Protein identification and quantification

Data were processed with Protein Pilot Software v. 5.0 (AB SCIEX) against a Haloxylon ammodendron database using the Paragon algorithm (Shilov et al. 2007). The experimental data from tandem mass spectrometry (MS) were used to match the theoretical data to identify proteins. The analysis was conducted using the National Center for Biotechnology Information (NCBI) FASTA database and UniProt protein database. Differentially accumulated proteins were classified according to GO (http://www.geneontology.org) and Kyoto Encyclopedia of Genes and Genomes (KEGG; http://www.genome.jp/kegg/ or http://www.kegg.jp/) categories to infer molecular functions, cellular components, biological processes, and significant pathways involved in response to cold stress.

Enzyme activity assays

The activities of superoxide dismutase (SOD) and peroxidase (POD) were assayed according to the procedure described by Wang and Huang (2015). Malate dehydrogenase (MDH) and glutathione peroxidase (GSH-Px) were measured according to the methods detailed by Zhu (1990) and Huang and Wu (1999), respectively.

qRT-PCR analysis

Total RNA was extracted from cold-treated and control A. aphylla seedlings using Trizol reagent (Takara, Shiga, Japan), and cDNA was reverse-transcribed using the Trans-Start Tip Green qPCR SuperMix (TransGen Biotech, Beijing, China). Gene-specific primers used for qRT-PCR, which were designed using primer3 according to the nucleic acid sequences obtained from the Haloxylon ammodendron database. The PCR reaction was carried out in a 10-μL reaction volume containing 5 μL of TransStart Tip Green qPCR SuperMix (TransGen Biotech), 1 μL of template, 0.25 μL of forward primer, 0.25 μL of reverse primer, and 3.5 μL of ddH$_2$O with thermal cycling conditions of 94°C for 30 s, followed by 40 cycles of 94°C for 5 s, 60°C for 30 s, and 20°C for 10 s.

Results

Primary data analysis and protein identification

Mascot identified a total of 525,160 spectra generated by the iTRAQ experiment. Of these, 138,117 spectra matched known spectra, with 28,341 unique peptides, and 4145 proteins on the basis of the applied >0.05 (10%) cutoff (Figure 1). The distribution of the number of peptides defining each protein is shown in Figure 2. More than 75% of the proteins included at least two peptides. GO annotation and KEGG analyses were carried out to identify the roles of the differentially accumulated proteins, and the results are shown in Figure 3.
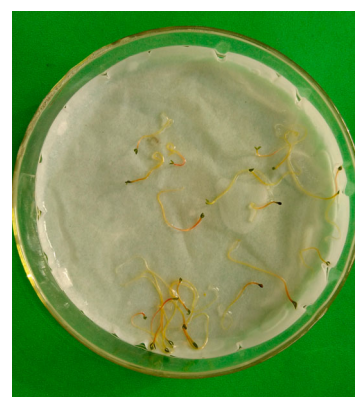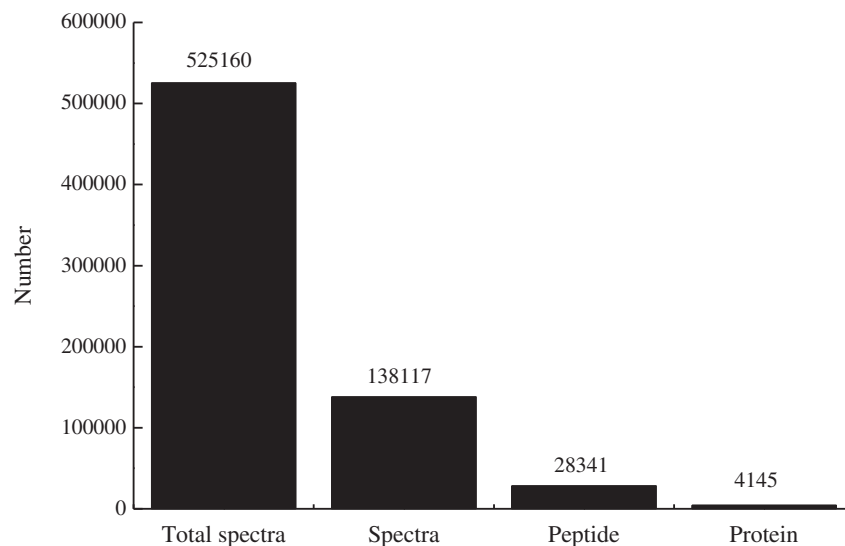
Figure 1. Spectra, peptides, and proteins identified via the iTRAQ proteomics technique after searching against the sequence databases.

Identification of differentially accumulated protein species by iTRAQ

Protein species were selected according to two criteria: $\geq 1.5 \times$ fold change and p-value <0.05. Based on these criteria, 211 differentially accumulated proteins were identified in *A. aphylla* seedlings, 109 of which were up-accumulated and 102 were down-accumulated under cold-stress conditions (Table 1). The main biological functions for the 211 differentially proteins were carbohydrate and energy metabolism, protein metabolic process, stress response, transcription-related, amino acid metabolism, signal transduction, and membrane and transport. Among them, some proteins, such as fructose-bisphosphate protein, glyceraldehyde-3-phosphate dehydrogenase, pyruvate kinase, citrate synthase, MDH, glucose dehydrogenase (GDH), photosynthesis protein, adenylate kinase (AK), ribosomal protein, elongation factor, heat shock protein, enzyme scavenging system proteins, TOPLESS protein, acetolactate synthase, glycine decarboxylase, membrane protein, channel protein, and transporter protein, were determined to be involved in these biological processes (these proteins are further highlighted in the section 'Discussion'). In addition, we found 26 proteins involved in unknown biological processes. Detailed information is shown in Figure 4.

Analysis of differentially expressed enzymes

Reactive oxygen species (ROS)-scavenging antioxidant mechanisms play an important role in maintaining suitable concentrations of ROS (Hasanuzzaman et al. 2012). To validate some of the DEPs, four enzymes involved in ROS scavenging and carbohydrate metabolism were selected for enzymatic activity analysis. The activities of SOD, MDH, and GSH-Px enzymes were increased by cold stress compared with the control treatment, though POD activity was decreased in the cold-stress treatment (Figure 5). These data corresponded with consistent trends in the iTRAQ results.

Transcriptional expression analysis by qRT-PCR

In order to elucidate the correlation in expression level between the mRNA and protein species, the expression levels
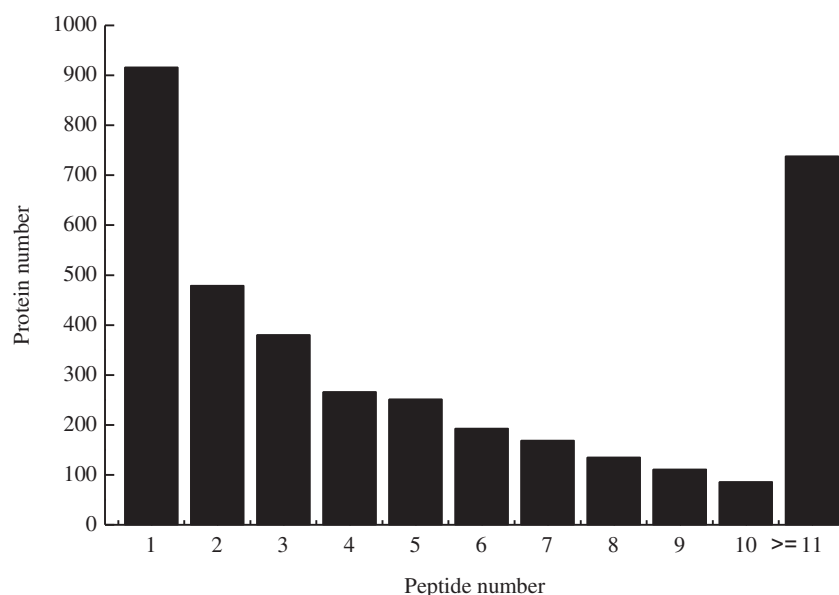

Figure 2. Number of peptides that were matched to proteins using MASCOT.
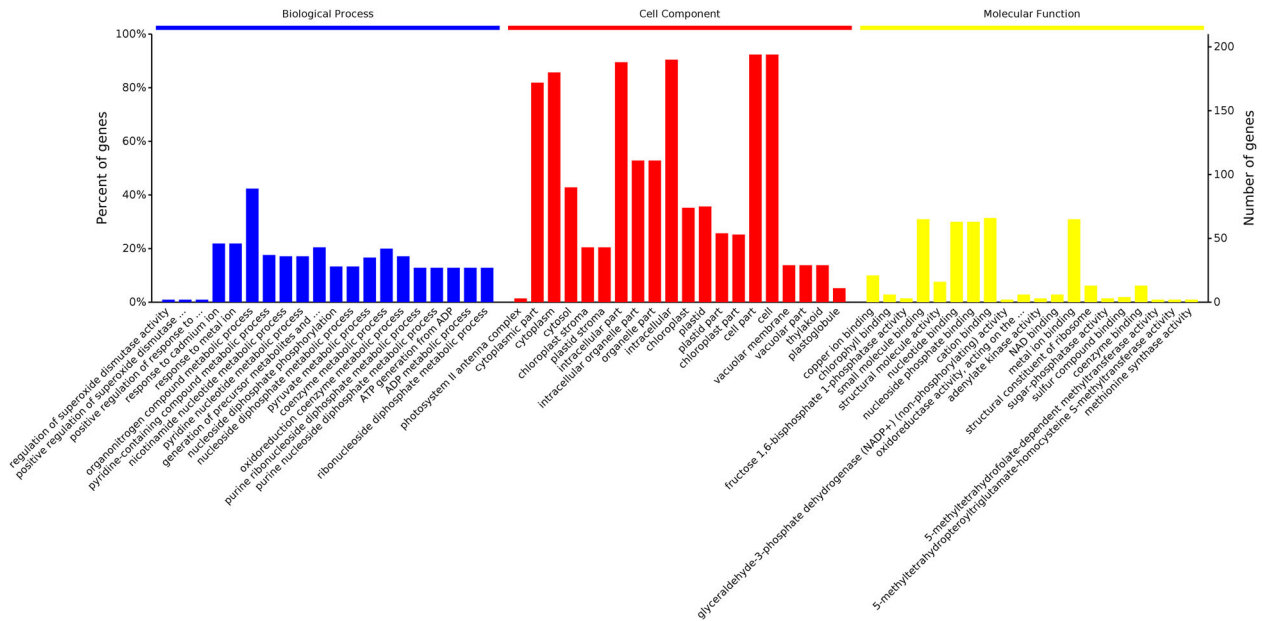
Figure 3. Gene ontology (GO) annotation of the differentially abundant proteins in cold-stress-treated *A. aphylla*.

of the transcripts corresponding to nine proteins were validated by qRT-PCR (Figure 6). The expression of eight transcripts was consistent with the abundance of the corresponding protein species including photosystem proteins, peroxiredoxin Q, and some ribosomal proteins (RPs). This indicated that the accumulation of these proteins is associated with mRNA transcript levels. However, the transcript expression assay for one of the proteins showed a trend that contrasted with the increased protein abundance, accordingly, this change in protein levels may have been caused by various posttranslational modifications such as glycosylation, protein phosphorylation, and ubiquitination under cold stress, rather than increased transcription.

Discussion

Carbohydrate and energy metabolism

Cold stress has a substantial effect on the abundance of proteins involved in carbohydrate and energy metabolism processes such as glycolysis, the TCA cycle, and the pentose phosphate pathway (PPP) in *A. aphylla* seedlings. In our study, the abundance of fructose-bisphosphate proteins (FBPs) was increased under cold stress. FBP aldolase is a key enzyme in glycolytic metabolism, and it catalyzes 1,6-fructose diphosphate into dihydroxyacetone phosphate and glyceraldehyde 3-phosphate. Excessive expression of FBP has been reported as a defense against abiotic stresses in *Arabidopsis* (Lu et al. 2012). Glyceraldehyde-3-phosphate dehydrogenase catalyzes glyceraldehyde 3-phosphate to 1,3-diphosphoglycerate. Pyruvate kinase catalyzes phosphoenolpyruvate and ADP into ATP and pyruvic acid. Glyceraldehyde-3-phosphate dehydrogenase and pyruvate kinase play important roles in the glycolysis pathways, and both of these two proteins were up-accumulated under cold stress. In other desert plants, namely *Populus euphratica* and *Ammopiptanthus mongolicus*, researchers also found that glyceraldehyde-3-phosphate dehydrogenase was up-accumulated, thus likely altering cold-stress resistant (Yue et al. 2009; Zhou et al. 2016), in agreement with our research.

Citrate synthase is an enzyme that controls the TCA cycle, in which it is the rate-limiting factor. In our results, the abundance of citrate synthase was down-accumulated under cold stress, which was consistent with a previous report on *Capsicum annuum* (Sánchez-Be et al. 2012). MDH catalyzes malic acid to oxaloacetate, after which oxaloacetate enters the TCA cycle, the abundance of this enzyme increased under cold stress in our data. Measured levels of MDH activity were also consistent with this result, indicating that the TCA cycle was inhibited in *A. aphylla* seedlings after cold-stress treatment.

Three proteins related to PPP were identified by the iTRAQ technique in our results: GDH, UTP-glucose-1-phosphate uridylyltransferase, and 6-phosphogluconolactonase. GDH is a key regulatory enzyme of the PPP, and its accumulation was enhanced under cold stress. However, both UTP-glucose-1-phosphate uridylyltransferase and 6-phosphogluconolactonase, which are involved in the PPP, were down-accumulated in our study. Differential protein accumulation of proteins involved in this metabolic pathway suggested that complicated regulation mechanisms respond to cold stress in *A. aphylla* seedlings.

Cold can also affect different aspects of photosynthesis significantly. Our proteomics results indicated that most of the proteins involved in photosynthesis were down-accumulated under cold stress. The down-accumulated proteins included the chloroplast chlorophyll A–B binding protein, photosystem II CP43 chlorophyll apoprotein, photosystem II protein D1, photosystem I P700 apoprotein A2 chain f, and the crystal structure of plant photosystem protein. Among these proteins, photosystem I P700 apoprotein A2 and photosystem II CP43 chlorophyll apoprotein reflected the overall trend observed in the qRT-PCR experiment. Chloroplast chlorophyll A–B binding protein was also differentially expressed in *Populus euphratica* (Yue et al. 2009). Similarly, an up-accumulated protein was identified in our data, namely oxygen-evolving enhancer protein 1. This result disagreed with a previously conducted expression profile of this protein in maize (Wang et al. 2016). Accordingly, *A. aphylla* seedlings may physiologically adapt to cold stress, in part, through changes in photosynthesis.

Table 1. Differential protein species between chilling stress and control conditions in *A. aphylla* seedlings by iTRAQ.

Accession no.	% Cov	Peptides (95%)	Protein species name	Species	Foldchange	Up/down
Carbohydrate and energy metabolism						
gi|226358407	56.7	20	Chloroplast chlorophyll A–B binding protein	*Gossypium hirsutum*	0.6161	↓
gi|350538149	24.9	10	Chloroplast sedoheptulose-1,7-bisphosphatase	*Solanum lycopersicum*	0.6627	↓
gi|910354439	33.6	26	Photosystem II CP43 chlorophyll apoprotein (chloroplast)	*Haloxylon persicum*	0.6049	↓
gi|91208882	23	11	Photosystem II protein D1 (chloroplast)	*Gossypium hirsutum*	0.5868	↓
gi|910354442	19.8	13	Photosystem I P700 apoprotein A2 (chloroplast)	*Haloxylon persicum*	0.6532	↓
gi|829581677	31.8	7	Chain f, Crystal Structure Of Plant Photosystem I-lhci Super-complex At 2.8 Angstrom Resolution		0.5961	↓
gi|910354501	32.4	8	NADH-plastoquinone oxidoreductase subunit 7 (chloroplast)	*Haloxylon persicum*	0.6397	↓
gi|700193260	41.9	16	Oxygen-evolving enhancer protein 1	*Cucumis sativus*	1.5090	↑
gi|78191470	18.5	7	Fructokinase-like	*Solanum tuberosum*	0.4929	↓
gi|533055962	24.9	5	Fructose-1,6-bisphosphatase	*Gossypium hirsutum*	0.1416	↓
gi|460375513	27.9	17	PREDICTED: fructose-bisphosphate aldolase 1, chloroplastic-like	*Solanum lycopersicum*	1.5044	↑
gi|460408038	28.2	11	PREDICTED: fructose-bisphosphate aldolase cytoplasmic isozyme-like	*Solanum lycopersicum*	2.6314	↑
gi|831360236	16.4	2	Probable 6-phosphogluconolactonase 4, chloroplastic	*Solanum lycopersicum*	0.6450	↓
gi|460409628	30.6	13	PREDICTED: UTP--glucose-1-phosphate uridylyltransferase isoform X1	*Solanum lycopersicum*	0.6437	↓
gi|211906438	50.5	27	UDP-D-glucose dehydrogenase	*Gossypium hirsutum*	4.9353	↑
gi|723754550	28.5	3	PREDICTED: NADH-ubiquinone oxidoreductase chain 1	*Solanum lycopersicum*	2.6599	↑
gi|743943692	20	9	PREDICTED: ATP synthase subunit gamma, mitochondrial-like	*Populus euphratica*	2.1312	↑
gi|460366958	24.3	7	PREDICTED: citrate synthase, mitochondrial	*Solanum lycopersicum*	0.3959	↓
gi|460380474	31.8	12	PREDICTED: malate dehydrogenase, chloroplastic-like	*Solanum lycopersicum*	1.5140	↑
gi|460381200	32.8	6	PREDICTED: adenylate kinase 4	*Solanum lycopersicum*	1.7093	↑
gi|460387035	28.1	5	PREDICTED: adenylate kinase 4	*Solanum lycopersicum*	2.1960	↑
gi|460402152	15.4	6	PREDICTED: pyruvate kinase, cytosolic isozyme	*Solanum lycopersicum*	0.3294	↓
gi|460391793	58.2	55	PREDICTED: glyceraldehyde-3-phosphate dehydrogenase, cytosolic	*Solanum lycopersicum*	0.6384	↓
gi|806776532	54.4	30	Glyceraldehyde-3-phosphate dehydrogenase	*Solanum lycopersicum*	0.4486	↓
gi|723658980	20.7	27	PREDICTED: pyruvate, phosphate dikinase, chloroplastic	*Solanum lycopersicum*	0.5676	↓
gi|778682516	13.3	7	PREDICTED: alanine aminotransferase 2-like isoform X2	*Cucumis sativus*	0.3675	↓
gi|728839885	14.8	7	Formate--tetrahydrofolate ligase	*Gossypium arboreum*	1.5707	↑
gi|460391381	54.9	17	PREDICTED: UDP-D-apiose/UDP-D-xylose synthase 2-like	*Solanum lycopersicum*	1.7888	↑
gi|778690463	15.9	7	PREDICTED: inositol-3-phosphate synthase-like	*Cucumis sativus*	1.6143	↑
gi|902222029	27	20	Hypothetical protein SOVF_064910	*Spinacia oleracea*	1.8624	↑
gi|902217466	42.9	20	Hypothetical protein SOVF_077450	*Spinacia oleracea*	2.0868	↑
gi|902173153	83.4	43	Hypothetical protein SOVF_164510	*Spinacia oleracea*	2.3710	↑
gi|902186880	26	9	Hypothetical protein SOVF_140950	*Spinacia oleracea*	0.6458	↓
gi|902226097	33.5	8	Hypothetical protein SOVF_053890	*Spinacia oleracea*	1.9612	↑
gi|902208123	57.6	11	Hypothetical protein SOVF_094420	*Spinacia oleracea*	2.3406	↑
gi|902201718	20.2	8	Hypothetical protein SOVF_111130	*Spinacia oleracea*	0.5582	↓
gi|902166152	23.1	5	Hypothetical protein SOVF_174110	*Spinacia oleracea*	1.9808	↑
gi|700205640	40.1	22	Hypothetical protein Csa_2G009470	*Cucumis sativus*	0.6049	↓
gi|902198413	28.6	13	Hypothetical protein SOVF_114690	*Spinacia oleracea*	1.8010	↑
gi|902234721	18.5	8	Hypothetical protein SOVF_023640	*Spinacia oleracea*	0.5488	↓
gi|902194849	26.3	8	Hypothetical protein SOVF_123870	*Spinacia oleracea*	1.8445	↑
gi|902211583	13.6	3	Hypothetical protein SOVF_086270	*Spinacia oleracea*	1.7172	↑
gi|902166551	19.2	3	Hypothetical protein SOVF_173630	*Spinacia oleracea*	1.5621	↑
gi|902238839	8.3	5	Hypothetical protein SOVF_007440	*Spinacia oleracea*	0.5011	↓
gi|902231300	12.6	3	Hypothetical protein SOVF_036130	*Spinacia oleracea*	0.5358	↓
gi|902218113	9.9	7	Hypothetical protein SOVF_075180	*Spinacia oleracea*	1.5803	↑
gi|902235043	28	9	Hypothetical protein SOVF_022510	*Spinacia oleracea*	0.5463	↓
gi|902165738	12.8	3	Hypothetical protein SOVF_174610	*Spinacia oleracea*	0.5500	↓
gi|700199184	27.9	8	Hypothetical protein Csa_4G307350	*Cucumis sativus*	0.6271	↓
gi|700196117	55.7	84	Hypothetical protein Csa_5G514500	*Cucumis sativus*	1.7332	↑

gi|902167268	14.5	2	Hypothetical protein SOVF_172700	*Spinacia oleracea*	0.5262	↓
gi|902153533	9.7	6	Hypothetical protein SOVF_187820	*Spinacia oleracea*	1.9776	↑
gi|902190453	10.6	2	Hypothetical protein SOVF_133530	*Spinacia oleracea*	1.5153	↑
gi|902236844	8.2	3	Hypothetical protein SOVF_014560	*Spinacia oleracea*	0.2360	↓
gi|902166108	5.6	2	Hypothetical protein SOVF_174150	*Spinacia oleracea*	0.4368	↓
gi|902239307	13	4	Hypothetical protein SOVF_005810	*Spinacia oleracea*	0.6687	↓
gi|700187952	22	8	Hypothetical protein Csa_7G007830	*Cucumis sativus*	0.3001	↓
gi|902184516	67.6	37	Hypothetical protein SOVF_145640	*Spinacia oleracea*	0.6646	↓
gi|902157669	45.4	12	Hypothetical protein SOVF_183590	*Spinacia oleracea*	0.3844	↓
gi|700188155	32.3	10	Hypothetical protein Csa_7G030510	*Cucumis sativus*	0.6568	↓
gi|902203804	31.3	8	Hypothetical protein SOVF_104460	*Spinacia oleracea*	1.5799	↑
gi|700188288	40.6	28	Hypothetical protein Csa_7G043630	*Cucumis sativus*	0.4830	↓
gi|902186385	17.7	8	Hypothetical protein SOVF_142190	*Spinacia oleracea*	1.5778	↑
gi|902210584	16.5	3	Hypothetical protein SOVF_088830	*Spinacia oleracea*	1.8624	↑
gi|902172866	22.3	10	Hypothetical protein SOVF_164960	*Spinacia oleracea*	1.5807	↑
gi|700190947	31.4	10	Hypothetical protein Csa_6G057170	*Cucumis sativus*	1.7189	↑
gi|902157684	25.2	9	Hypothetical protein SOVF_183760	*Spinacia oleracea*	1.8499	↑
gi|902232594	32.1	9	Hypothetical protein SOVF_031810	*Spinacia oleracea*	0.6284	↓
gi|700193023	26.5	9	Hypothetical protein Csa_6G449830	*Cucumis sativus*	0.3091	↓
gi|902183996	35.9	14	Hypothetical protein SOVF_146400	*Spinacia oleracea*	0.5929	↓
gi|902210014	67.9	65	Hypothetical protein SOVF_090230	*Spinacia oleracea*	0.6232	↓
gi|902190671	15.7	7	Hypothetical protein SOVF_133140	*Spinacia oleracea*	1.5622	↑
gi|902211963	13.1	3	Hypothetical protein SOVF_085120	*Spinacia oleracea*	3.9962	↑
Protein metabolic process						
gi|910354482	36.7	8	Ribosomal protein S3 (chloroplast)	*Haloxylon persicum*	0.5710	↓
gi|910354445	44.8	7	Ribosomal protein S4 (chloroplast)	*Haloxylon persicum*	0.6677	↓
gi|910354432	44.9	5	Ribosomal protein S2 (chloroplast)	*Haloxylon persicum*	0.4654	↓
gi|7636087	40.9	3	Ribosomal protein S16 (chloroplast)	*Spinacia oleracea*	0.4818	↓
gi|728823057	16.4	5	30S ribosomal 1, chloroplastic	*Gossypium arboreum*	1.7417	↑
gi|460413795	35	2	PREDICTED: 40S ribosomal protein S19-3	*Solanum lycopersicum*	0.3637	↓
gi|525314400	39.1	10	Phosphate carrier protein, mitochondrial-like	*Solanum lycopersicum*	0.4241	↓
gi|460411113	46.6	58	PREDICTED: heat shock cognate 70 kDa protein	*Solanum lycopersicum*	1.7768	↑
gi|743929745	17.4	2	PREDICTED: 10 kDa chaperonin-like	*Populus euphratica*	0.6399	↓
gi|460410622	35.5	4	PREDICTED: SKP1-like protein 1A	*Solanum lycopersicum*	0.3670	↓
gi|778675929	6.1	3	PREDICTED: fimbrin-1	*Cucumis sativus*	2.1824	↑
gi|460379690	20.9	3	PREDICTED: chaperonin CPN60-like 2, mitochondrial	*Solanum lycopersicum*	0.4795	↓
gi|778714609	30.5	4	PREDICTED: outer envelope pore protein 16-2, chloroplastic	*Cucumis sativus*	0.5127	↓
gi|778717063	6.8	2	PREDICTED: dnaJ protein P58IPK homolog isoform X2	*Cucumis sativus*	1.8073	↑
gi|460395617	19.9	15	PREDICTED: 26S proteasome non-ATPase regulatory subunit 2 homolog A	*Solanum lycopersicum*	0.6516	↓
gi|460372323	11.3	7	PREDICTED: probable cytosolic oligopeptidase A	*Solanum lycopersicum*	1.5076	↑
gi|723724297	20.7	24	PREDICTED: puromycin-sensitive aminopeptidase isoform X2	*Solanum lycopersicum*	1.7094	↑
gi|756179878	47.9	11	Chloroplast M-type thioredoxin	*Suaeda glauca*	1.5293	↑
gi|778657028	10.9	3	PREDICTED: H/ACA ribonucleoprotein complex subunit 4	*Cucumis sativus*	1.8074	↑
gi|74486738	58.6	61	Translation elongation factor 1A-6	*Gossypium hirsutum*	1.6067	↑
gi|743938152	52.2	64	PREDICTED: elongation factor 2	*Populus euphratica*	0.4165	↓
gi|460383656	8.2	3	PREDICTED: dipeptidyl-peptidase 5-like	*Solanum lycopersicum*	0.5155	↓
gi|902237664	68.2	54	Hypothetical protein SOVF_011500	*Spinacia oleracea*	1.6078	↑
gi|902219823	28.1	15	Hypothetical protein SOVF_070690	*Spinacia oleracea*	1.6014	↑
gi|700197689	66.3	14	Hypothetical protein Csa_4G003610	*Cucumis sativus*	2.7070	↑
gi|902206403	52.2	17	Hypothetical protein SOVF_097960	*Spinacia oleracea*	1.6722	↑
gi|902221763	49.6	11	Hypothetical protein SOVF_065570	*Spinacia oleracea*	1.5391	↑
gi|902163232	45.2	18	Hypothetical protein SOVF_177720	*Spinacia oleracea*	1.5339	↑
gi|902231423	26.4	15	Hypothetical protein SOVF_035670	*Spinacia oleracea*	2.0685	↑
gi|902217954	33.2	5	Hypothetical protein SOVF_075470	*Spinacia oleracea*	1.8125	↑

Table 1. Continued.

Accession no.	% Cov	Peptides (95%)	Protein species name	Species	Foldchange	Up/down
gi|902207733	8.9	4	Hypothetical protein SOVF_095160	*Spinacia oleracea*	1.8806	↑
gi|700188118	35.2	3	Hypothetical protein Csa_7G025720	*Cucumis sativus*	2.4145	↑
gi|902160928	51.6	4	Hypothetical protein SOVF_180190	*Spinacia oleracea*	2.0258	↑
gi|700198902	23.8	9	Hypothetical protein Csa_4G279880	*Cucumis sativus*	1.5371	↑
gi|700191656	32.4	20	Hypothetical protein Csa_6G147530	*Cucumis sativus*	2.0274	↑
gi|902198669	34.7	9	Hypothetical protein SOVF_114060	*Spinacia oleracea*	1.8632	↑
gi|902210705	43.3	4	Hypothetical protein SOVF_088520	*Spinacia oleracea*	1.7384	↑
gi|902218457	17	9	Hypothetical protein SOVF_074530	*Spinacia oleracea*	0.5710	↓
gi|902188498	17.1	3	Hypothetical protein SOVF_137230	*Spinacia oleracea*	1.6494	↑
gi|902178639	9.5	2	Hypothetical protein SOVF_155830	*Spinacia oleracea*	1.6346	↑
gi|902219714	9.4	2	Hypothetical protein SOVF_070750	*Spinacia oleracea*	0.4679	↓
gi|902230746	40.5	12	Hypothetical protein SOVF_038440	*Spinacia oleracea*	1.5826	↑
gi|902233956	39.9	5	Hypothetical protein SOVF_026510	*Spinacia oleracea*	2.5890	↑
gi|902186125	15.9	7	Hypothetical protein SOVF_142670	*Spinacia oleracea*	0.5169	↓
gi|902153461	6.2	2	Hypothetical protein SOVF_187920	*Spinacia oleracea*	1.5079	↑
gi|700202381	22.8	8	Hypothetical protein Csa_3G202720	*Cucumis sativus*	1.7376	↑
gi|700205858	20.2	8	Hypothetical protein Csa_2G033320	*Cucumis sativus*	0.5763	↓
gi|902194727	27.2	14	Hypothetical protein SOVF_124230, partial	*Spinacia oleracea*	0.5505	↓
Stress response						
gi|363818265	42.7	13	Choline monooxygenase	*Haloxylon persicum*	1.7628	↑
gi|373839258	45	19	Peroxiredoxin Q	*Haloxylon ammodendron*	0.6320	↓
gi|2832921	26.9	11	Stromal ascorbate peroxidase	*Spinacia oleracea*	0.5458	↓
gi|90823174	33.6	3	Putative cytosolic copper/zinc superoxide dismutase	*Gossypium hirsutum*	2.9112	↑
gi|460403245	18	10	PREDICTED: 3-ketoacyl-CoA thiolase 2, peroxisomal	*Solanum lycopersicum*	1.5665	↑
gi|460414473	16.5	5	PREDICTED: probable glutathione peroxidase 8	*Solanum lycopersicum*	2.2455	↑
gi|946577364	15.4	5	Phosphoethanolamine N-methyltransferase	*Spinacia oleracea*	1.5452	↑
gi|50399950	13.8	5	Putative Lysyl-tRNA synthetase	*Oryza sativa Japonica Group*	0.6100	↓
gi|970414516	26.6	8	V-type proton ATPase subunit E	*Solanum lycopersicum*	2.0250	↑
gi|778683189	18.7	4	PREDICTED: acyl-coenzyme A oxidase 4, peroxisomal isoform X2	*Cucumis sativus*	0.6310	↓
gi|400404	33.8	11	RecName: Full = Nucleoside diphosphate kinase 1; AltName: Full = Nucleoside diphosphate kinase I; Short = NDK I; Short = NDP kinase I; Short = NDPK I	SPIOL	1.6424	↑
gi|823683802	38.2	18	S-adenosylmethionine synthase 2	*Solanum lycopersicum*	2.1122	↑
gi|460369292	29.2	8	PREDICTED: ankyrin repeat domain-containing protein 2	*Solanum lycopersicum*	1.6567	↑
gi|756179888	16.3	3	Chloroplast ATP synthase delta	*Suaeda glauca*	2.0995	↑
gi|902117496	37.5	25	Hypothetical protein SOVF_204310	*Spinacia oleracea*	0.6232	↓
gi|902153503	22.5	7	Hypothetical protein SOVF_187860	*Spinacia oleracea*	0.6315	↓
gi|902190448	42	16	Hypothetical protein SOVF_133480	*Spinacia oleracea*	2.0035	↑
gi|902228007	57.1	5	Hypothetical protein SOVF_047880	*Spinacia oleracea*	0.6533	↓
gi|902235600	17.3	3	Hypothetical protein SOVF_020220	*Spinacia oleracea*	3.5609	↑
gi|902126118	10.9	4	Hypothetical protein SOVF_202790	*Spinacia oleracea*	1.7124	↑
gi|902233438	49.6	9	Hypothetical protein SOVF_028130	*Spinacia oleracea*	0.5590	↓
gi|902117209	12.9	3	Hypothetical protein SOVF_204400	*Spinacia oleracea*	0.5090	↓
gi|902161299	21.1	8	Hypothetical protein SOVF_179880, partial	*Spinacia oleracea*	0.3716	↓
gi|902224379	14.5	11	Hypothetical protein SOVF_058270	*Spinacia oleracea*	0.6538	↓
Transcription-related						
gi|778689635	14.1	10	PREDICTED: protein TOPLESS	*Cucumis sativus*	0.6422	↓
gi|723708372	11.2	3	PREDICTED: AP-1 complex subunit mu-2-like	*Solanum lycopersicum*	3.0510	↑
gi|743938334	15.7	5	PREDICTED: probable nucleolar protein 5-1	*Populus euphratica*	0.5725	↓
gi|902220349	26.7	34	Hypothetical protein SOVF_069380	*Spinacia oleracea*	1.6063	↑
gi|902234483	19.8	3	Hypothetical protein SOVF_024550	*Spinacia oleracea*	0.5348	↓
gi|902219770	24.1	6	Hypothetical protein SOVF_071080	*Spinacia oleracea*	2.1805	↑
gi|902233479	12.2	2	Hypothetical protein SOVF_028180	*Spinacia oleracea*	0.6215	↓
gi|902205013	4.1	3	Hypothetical protein SOVF_101730	*Spinacia oleracea*	0.6470	↓

gi|902217903	15.5	10	Hypothetical protein SOVF_075510	*Spinacia oleracea*	1.6525	↑

Amino acid metabolism

gi|778678626	22	6	PREDICTED: glutamine synthetase leaf isozyme, chloroplastic	*Cucumis sativus*	0.4869	↓
gi|460377776	10	3	PREDICTED: acetolactate synthase 2, chloroplastic	*Solanum lycopersicum*	1.5253	↑
gi|987996456	54.1	54	5-methyltetrahydropteroyltriglutamate--homocysteine methyltransferase	*Solanum lycopersicum*	0.6030	↓
gi|460365154	46.8	47	PREDICTED: 5-methyltetrahydropteroyltriglutamate--homocysteine methyltransferase	*Solanum lycopersicum*	0.5654	↓
gi|460399143	18.2	13	PREDICTED: glycine dehydrogenase (decarboxylating), mitochondrial	*Solanum lycopersicum*	0.6390	↓
gi|902208422	19.6	6	Hypothetical protein SOVF_093740	*Spinacia oleracea*	0.6497	↓
gi|902232575	30.3	13	Hypothetical protein SOVF_032150	*Spinacia oleracea*	0.6109	↓
gi|902208677	27.2	4	Hypothetical protein SOVF_093100	*Spinacia oleracea*	0.6645	↓
gi|902219682	63.9	58	Hypothetical protein SOVF_071300	*Spinacia oleracea*	1.8583	↑
gi|902235597	38.5	19	Hypothetical protein SOVF_019040	*Spinacia oleracea*	1.6242	↑
gi|902206670	19	5	Hypothetical protein SOVF_097520	*Spinacia oleracea*	0.6147	↓

Signal transduction

gi|778658864	13.8	2	PREDICTED: mitogen-activated protein kinase homolog NTF6	*Cucumis sativus*	2.1779	↑
gi|902131771	38.2	27	Hypothetical protein SOVF_201000	*Spinacia oleracea*	2.0759	↑
gi|902167310	40.6	7	Hypothetical protein SOVF_172660	*Spinacia oleracea*	1.5763	↑
gi|902231507	44.3	8	Hypothetical protein SOVF_034180	*Spinacia oleracea*	1.8507	↑
gi|902165459	44.9	7	Hypothetical protein SOVF_174910	*Spinacia oleracea*	1.7059	↑
gi|902231306	11.5	2	Hypothetical protein SOVF_036190	*Spinacia oleracea*	1.6223	↑
gi|902234716	54.7	31	Hypothetical protein SOVF_023600	*Spinacia oleracea*	1.5205	↑
gi|902209880	11.3	2	Hypothetical protein SOVF_090490	*Spinacia oleracea*	0.6636	↓

Membrane and transport

gi|559148734	19.9	8	Mitochondrial dicarboxylate transporter	*Suaeda glauca*	1.6553	↑
gi|743925462	4	4	PREDICTED: probable manganese-transporting ATPase PDR2	*Populus euphratica*	1.6692	↑
gi|460377193	22.9	5	PREDICTED: membrane steroid-binding protein 2-like	*Solanum lycopersicum*	0.1022	↓
gi|700206882	17	4	Porin/voltage-dependent anion-selective channel protein	*Cucumis sativus*	0.4368	↓
gi|700204454	23.8	11	Hypothetical protein Csa_3G827290	*Cucumis sativus*	1.6408	↑
gi|902189125	10.7	8	Hypothetical protein SOVF_136540	*Spinacia oleracea*	0.6421	↓
gi|902221417	5.6	3	Hypothetical protein SOVF_066330	*Spinacia oleracea*	0.6685	↓
gi|902200852	35.5	8	Hypothetical protein SOVF_113000	*Spinacia oleracea*	0.6006	↓
gi|700192185	59.6	8	Hypothetical protein Csa_6G309960	*Cucumis sativus*	2.5402	↑
gi|902208624	8.2	3	Hypothetical protein SOVF_093240	*Spinacia oleracea*	0.5742	↓
gi|700193414	20.5	2	Hypothetical protein Csa_6G495720	*Cucumis sativus*	0.5831	↓
gi|902225030	39.6	13	Hypothetical protein SOVF_056850	*Spinacia oleracea*	1.6194	↑

Unknown

gi|723713849	8.7	2	PREDICTED: uncharacterized protein LOC101254708	*Solanum lycopersicum*	0.5970	↓
gi|902159441	16.2	10	Hypothetical protein SOVF_182050 isoform B	*Spinacia oleracea*	0.6050	↓
gi|902170106	40.1	14	Hypothetical protein SOVF_168790	*Spinacia oleracea*	1.5163	↑
gi|902190159	61.7	46	Hypothetical protein SOVF_134140	*Spinacia oleracea*	1.6101	↑
gi|902207477	18.1	10	Hypothetical protein SOVF_095650	*Spinacia oleracea*	0.6615	↓
gi|902202643	50.6	41	Hypothetical protein SOVF_108460	*Spinacia oleracea*	1.6532	↑
gi|902234906	38.3	9	Hypothetical protein SOVF_023050	*Spinacia oleracea*	0.6372	↓
gi|902162500	44.3	6	Hypothetical protein SOVF_178690 isoform B	*Spinacia oleracea*	0.6148	↓
gi|902221849	13.2	4	Hypothetical protein SOVF_065100	*Spinacia oleracea*	2.1508	↑
gi|902163135	10.4	4	Hypothetical protein SOVF_177920 isoform B	*Spinacia oleracea*	0.5044	↓
gi|902229215	64.3	18	Hypothetical protein SOVF_043360 isoform B	*Spinacia oleracea*	2.0668	↑
gi|902191568	20.1	7	Hypothetical protein SOVF_131100	*Spinacia oleracea*	0.6318	↓
gi|902191383	13.7	9	Hypothetical protein SOVF_131310 isoform B	*Spinacia oleracea*	0.5253	↓
gi|902224967	9.8	5	Hypothetical protein SOVF_056920 isoform B, partial	*Spinacia oleracea*	2.0551	↑
gi|700208755	49.5	15	Hypothetical protein Csa_1G024830	*Cucumis sativus*	0.6292	↓
gi|902212732	34.8	15	Hypothetical protein SOVF_083420 isoform B	*Spinacia oleracea*	1.5671	↑
gi|902183216	18.2	6	Hypothetical protein SOVF_147710 isoform B	*Spinacia oleracea*	0.5439	↓
gi|902189878	44.1	6	Hypothetical protein SOVF_134730	*Spinacia oleracea*	2.8363	↑

Table 1. Continued.

Accession no.	% Cov	Peptides (95%)	Protein species name	Species	Foldchange	Up/down
gi|902237480	8	4	Hypothetical protein SOVF_012280	Spinacia oleracea	1.6657	↑
gi|902095864	11.3	2	Hypothetical protein SOVF_209360	Spinacia oleracea	0.3167	↓
gi|902238083	28.2	4	Hypothetical protein SOVF_010000 isoform B	Spinacia oleracea	0.6008	↓
gi|902138670	7.8	4	Hypothetical protein SOVF_198990, partial	Spinacia oleracea	3.9875	↑
gi|902202339	31	6	Hypothetical protein SOVF_109340	Spinacia oleracea	1.6051	↑
gi|902194434	10.8	2	Hypothetical protein SOVF_124660	Spinacia oleracea	1.6639	↑
gi|902175112	12.4	2	Hypothetical protein SOVF_161780	Spinacia oleracea	1.5317	↑
gi|902228854	12.4	3	Hypothetical protein SOVF_044600	Spinacia oleracea	0.5333	↓

AK plays a key role in maintaining the balance of cell energy. As a protein kinase, AK catalyzes AMP to ADP while an organism is at a low energy level. ADP is oxidized into ATP, which is the direct supplier of energy in organisms through oxidative phosphorylation, thereby ensuring the normal vital activities of organisms (Lai et al. 2001). As such, the accumulation of AK may affect the level of ADP or ATP. Two AK proteins in our results were up-accumulated, suggesting that *A. aphylla* seedlings resist cold stress by storing additional energy.

Most proteins related to catabolism were also up-accumulated, whereas most of the photosynthesis proteins were down-accumulated under cold stress, which is consistent with a previous report on *Chorispora bungeana* (Sun 2011). This may be a consequence of cold affecting the activity of various photosynthetic enzymes in the chloroplast, thus resulting in the degradation of many important photosynthetic proteins. In order to survive, plants need more energy to sustain their life activities through processes such as catabolism and in this way to adapt cold stress.

Protein metabolism

Proteins are involved in the regulation of various metabolic activities in organisms, including the processes of translation, digestion, folding, and degradation in plants (Reinbothe et al. 2010). We identified several proteins that are involved in protein metabolism using the iTRAQ data. We found eight DEPs related to protein synthesis, including six RPs and two elongation factors. RPs are essential for protein synthesis and have been revealed to play important roles in metabolism, cell division, and growth (Wang 2013). In our study, the abundance of five RPs decreased, while one increased. Among the RPs, the qRT-PCR validation results of ribosomal protein S2, ribosomal protein S3, and ribosomal protein S4 were consistent with the protein accumulation results. Several relevant studies have linked abundances of RPs to abiotic stress level. One previous study reported that some ribosomal protein expression levels decreased while other specific ribosomal components increased (Laura et al. 2011). Cheng et al. (2016) also showed some RPs related to protein processing were up- or down-accumulated under abiotic stress in two hemp varieties. Additionally, we found that the abundance of translation elongation factor 1A-6 was up-accumulated under cold stress. This elongation factor is an organelle protein that plays a central role in the elongation phase of protein synthesis. Conversely, the abundance of elongation factor 2 was down-accumulated under cold stress, indicating that the expression levels of different elongation factors respond differently to cold stress.

Heat shock proteins (HSPs) are ubiquitous protective proteins in plants. HSPs mainly act as a molecular chaperone to prevent protein denaturation and repair denatured proteins through binding with target proteins, which maintains the stability of plant internal environments, HSPs play a key role in plant development and stress-resistance processes (Li et al. 2016). In recent years, HSPs have been shown to increase dramatically in expression level under high temperatures, drought, peroxidation, and heavy metal stress (Wang et al. 2004). Under cold stress, the abundance of HSP70 was up-accumulated. Other proteins related to protein folding were also identified as differentially accumulated in our study, including 10 kDa chaperonin-like, chaperonin CPN60-like, cytosolic oligopeptidase A, and dnaJ protein
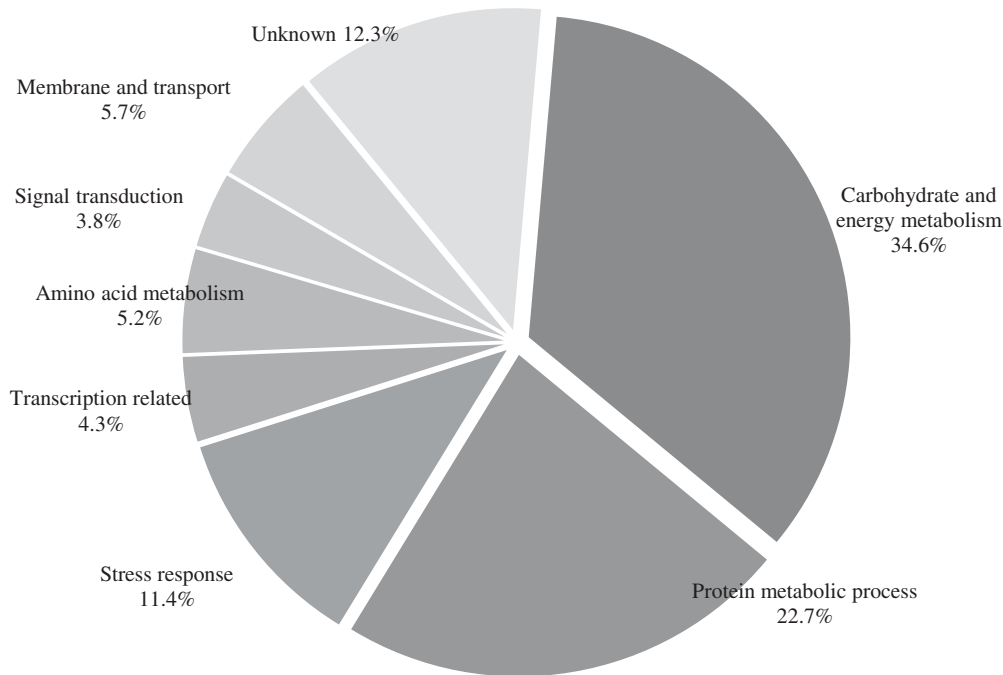
Figure 4. Functional classification of differentially accumulated *A. aphylla* proteins under cold stress.

P58IPK homolog isoform X2. Among these proteins, dnaJ is an accessory protein that enables ATP enzyme activity of HSP70, thereby regulating its activity, and it has a variety of functions, including folding new proteins, endocytosis, polypeptide transport via cell organelles, adjustments to stress responses, and the pre-degradation of protein targeting (Cyr et al. 1994; Krzysztof et al. 2008). Oligopeptidase may be involved in the degradation of proteasome-generated peptides with salicylic acid (Moreau et al. 2013). These two proteins were up-accumulated under cold stress, suggesting that the process of protein degradation increases with protein metabolism.

Stress response

Cold stress can cause excess production of ROS, which are important signal molecules in plants; however, ROS can also cause irreversible damage in plant cells (Asada 1999). In order to relieve cellular damage caused by ROS, plants have developed ROS-scavenging systems that include enzymatic scavenging systems, such as SOD, ascorbate peroxidase (APX), GSH-Px, SAM, and POD.

SOD is an enzyme that eliminates the harmful substances produced by metabolic processes. APX is considered to be a key enzyme in the detoxification of hydrogen peroxide in
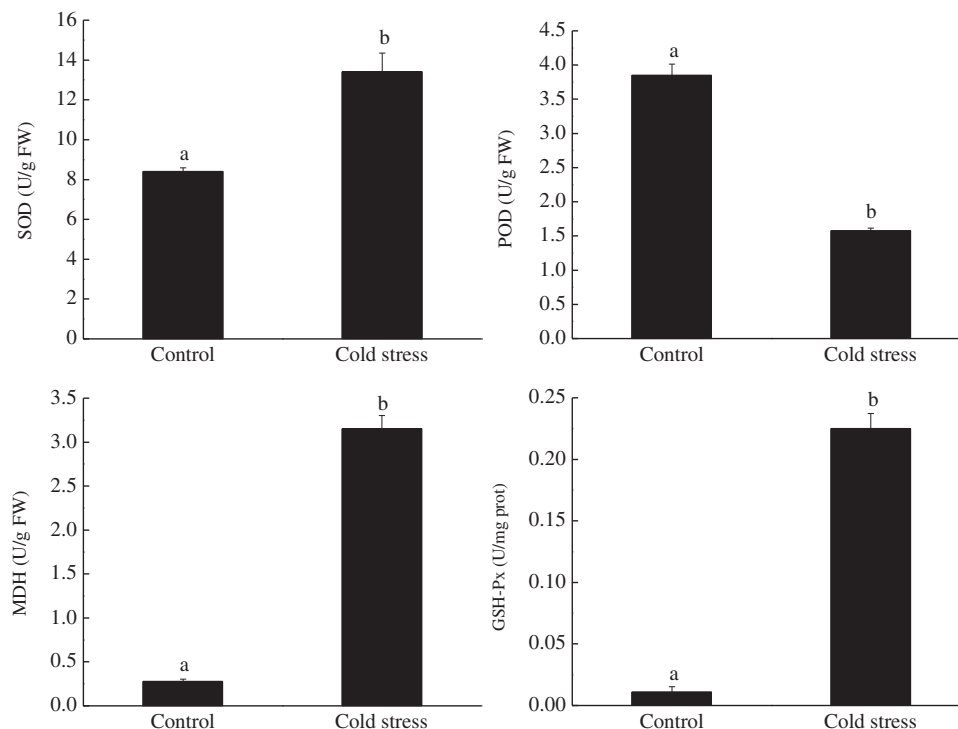

Figure 5. Activities of superoxide dismutase (SOD), peroxidase (POD), malate dehydrogenase (MDH), and glutathione peroxidase (GSH-Px) in *A. aphylla* under the control treatment and cold-stress treatment.
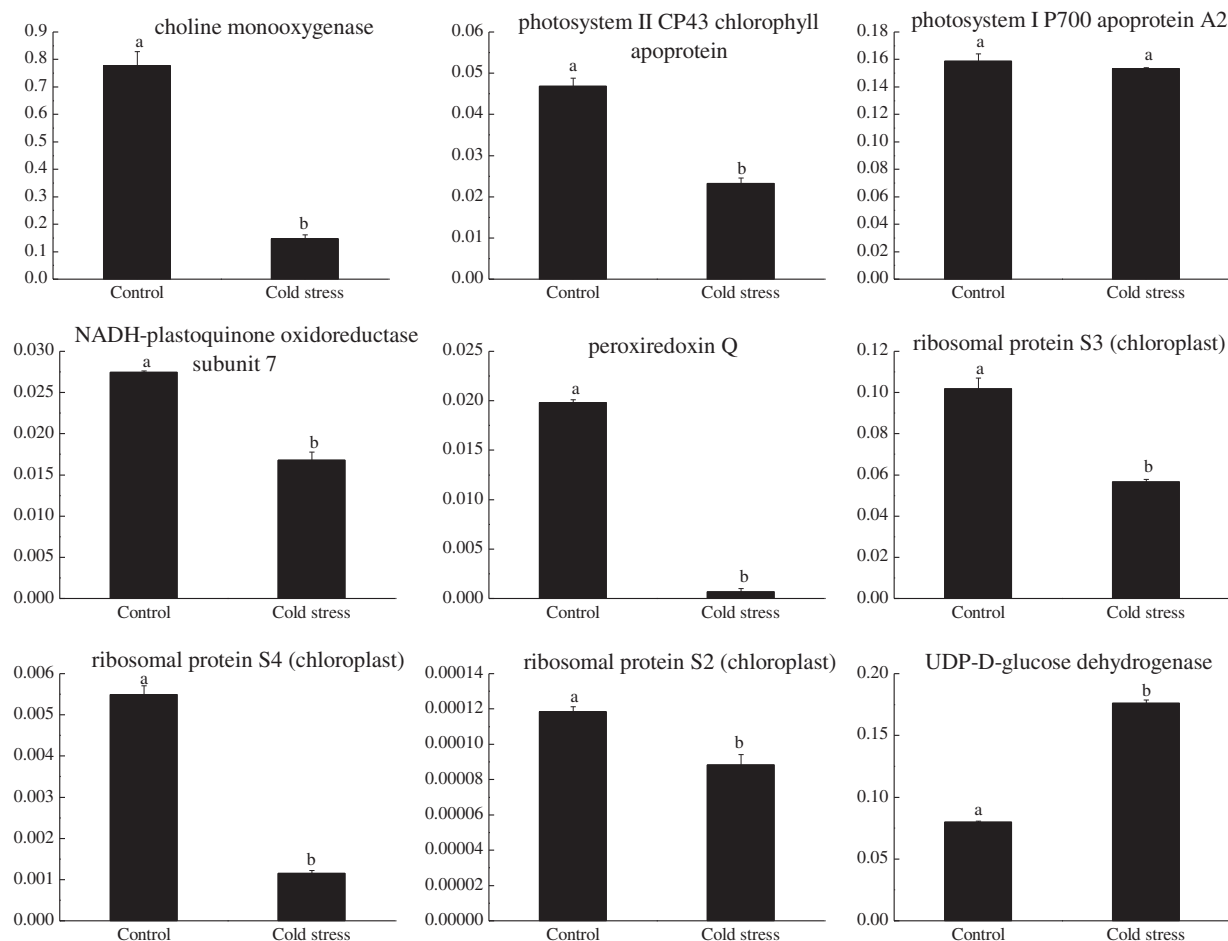
Figure 6. Analysis of transcript levels of the differentially accumulated *A. aphylla* proteins under the control and cold-stress treatments by qRT-PCR.

chloroplasts (Asada 1999). Under cold stress, the abundance of Cu/Zn SOD was increased, and this observation is consistent with the response of maize seedlings to cold stress in a previous study (Wang et al. 2016). APX showed overexpression in stressful conditions such as drought, cold, high salt, and heavy metal stress, enabling plant chloroplasts and mitochondria to resist stress caused by oxidative damage (Neilson et al. 2011). However, our results showed that the abundance of APX decreased under cold stress. Therefore, *A. aphylla* appears to resist cold through the accumulation of other antioxidant enzymes other than APX.

GSH-Px catalyzes glutathione into oxidized glutathione, enables the toxic peroxide reduction of nontoxic hydroxyl compounds, and promotes the decomposition of H_2O_2, thus protecting the structure and function of the cell membrane from interference and damage caused by peroxide (Nathalie et al. 1998). The increased abundance of GSH-Px under cold stress suggested that the protein helps cope with cold stress in *A. aphylla* seedlings. The GSH-Px enzyme activity assay also confirmed this finding.

POD is involved in respiration, photosynthesis, and the oxidation of auxin, its activity changes continuously in the process of plant growth and development (Zhao et al. 2013). In the present study, the POD isozyme levels decreased in response to cold stress, but the abundance of 3-ketoacyl-CoA thiolase 2, peroxisomal was increased. In previous studies, the abundance of POD increased under abiotic stress in wheat, barley, and cucumber, but decreased in creeping bentgrass (Peng et al. 2009; Witzel et al. 2009; Du et al. 2010; Xu et al. 2010). This suggested that the expression

mechanism of peroxidase in plants under cold stress is complex.

S-adenosylmethionine synthase catalyzes methionine and ATP into SAM, and S-adenosylmethionine synthase 2 is also a methyl donor. It participates in the synthesis of ethylene, polyamine, and plant hormones, substances that are closely linked to plant stress responses (Cui et al. 2005). The abundance of S-adenosylmethionine synthase 2 was increased under cold stress. Consistent with this observation, a previous study reported that S-adenosylmethionine synthase 2 was up-accumulated by cold stress in hybrid rice seedlings (Yan et al. 2006). Accordingly, the accumulation of antioxidant proteins may dissipate excess excitation energy and thus protect plant against cold stress.

Transcription and signal transduction

The regulation of transcription has great significance in the responses of plants to biotic and abiotic stresses (Jiang et al. 2007). The protein TOPLESS is a transcriptional corepressor that can repress the expression of root-promoting genes in the top half of the embryo to allow proper differentiation of the shoot pole during the transition stage of embryogenesis, it is also involved in the cellular synthesis of RNA on a template of DNA (Wei et al. 2015). A previous study has also shown that TOPLESS protein expression is related to transcription and stress response (Ke et al. 2015). In our data, TOPLESS was down-accumulated under cold stress. In *Arabidopsis*, the nucleolar protein is relevant to rRNA modification, which is vital in the response to abiotic stress

(Pendle et al. 2004). In our study, nucleolar protein decreased in abundance, suggesting that the down-accumulation of this protein in *A. aphylla* seedlings plays an important role in cold-stress response.

Mitogen-activated protein kinase homolog NTF6 is an enzyme that converts ATP to ADP and a phosphoprotein and is involved in the H_2O_2-mediated mitogen-activated protein kinase-signaling pathway. In our present study, mitogen-activated protein kinase homolog NTF6 showed higher accumulation levels, but in contrast, this protein showed downregulation in tobacco cells (Sasabe et al. 2006). This suggests that cold-resistant plants may physiologically adapt by altering signal transduction pathways.

Amino acid metabolism and membrane transport

As amino acids are the basic units of proteins and precursors for all protein production, their metabolism and availability have significant effects on plant growth, photosynthesis, and stress resistance (Yang et al. 2013). The protein 5-methyltetrahydropteroyltriglutamate-homocysteine methyltransferase catalyzes the transfer of a methyl group from 5-methyltetrahydrofolate to homocysteine resulting in methionine formation in L-methionine biosynthesis (Ravanel et al. 2004). Glycine dehydrogenase is involved in the glycine catabolic process and is also one of the key components of the glycine cleavage system (Palmieri et al. 2010). An abundance of glycine decarboxylase may generate more glutathione, a major antioxidant and free-radical scavenger in plants (Noctor et al. 1999; Foyer and Noctor 2000). Acetolactate synthase catalyzes the formation of acetolactate from pyruvate, and it is involved in the first step in valine and isoleucine biosynthesis (Mazur et al. 1987). This protein is also involved in the first steps of both the subpathway that synthesizes L-isoleucine from 2-oxobutanoate and the subpathway that synthesizes L-valine from pyruvate, which is part of amino acid biosynthesis. Both L-isoleucine and L-valine function in the repair of plant tissues and provide energy for plant growth (Wang et al. 2011). Under cold stress, the abundance of acetolactate synthase was increased, which suggested that the biosynthesis of L-isoleucine and L-valine had increased.

Membrane steroid-binding protein 2-like is an integral component of the membrane. Porin/voltage-dependent anion-selective channel protein is involved in transmembrane transport, an essential role in the maintenance of ion homeostasis in plant cells. Porin/voltage-dependent anion-selective channel protein was down-accumulated in our study as well as in a similar study conducted with cucumber (Huang et al. 2009). Manganese-transporting ATPase PDR2 mediates manganese transport into the endoplasmic reticulum, which is vital in pollen and root development through its impact on protein secretion and transport processes (Wang et al. 2008). Mitochondrial dicarboxylate transporter is an important transport protein in the inner membrane of chloroplasts. It catalyzes the exchange of dicarboxylic acids like malate and succinate for inorganic phosphate (Picault et al. 2002). These two transport proteins showed higher abundance in response to cold stress. They were induced in *Arabidopsis thaliana* and *Ananas comosus* (Kinoshita et al. 2011; Mirvat et al. 2016). As such, *A. aphylla* seedlings appear to adapt to the cold environments, in part, through alterations in their amino acid metabolism and membrane transport proteins.

Conclusion

A proteomics analysis using iTRAQ technology was performed to analyze differential protein accumulation under cold stress in *A. aphylla* seedlings. A total of 211 differentially accumulated proteins were identified between control and cold stress conditions seedlings, among which, 109 proteins were up-accumulated and 102 were down-accumulated. On the basis of GO and KEGG pathway enrichment analysis, we concluded that most of the proteins related to cold-stress response were involved in carbohydrate and energy metabolism, suggesting that *A. aphylla* seedlings primarily adapted to cold conditions through accumulations of proteins involved in energy metabolism pathways. In addition, proteins in some biological processes related to cold stress also had an effect on cold resistance of *A. aphylla* seedlings, including protein translation, transcriptional regulation, amino acid metabolism, signal transduction, and membrane transport. We also used qRT-PCR technique to confirm positive relationships in expression level between the mRNA transcript and protein species. These results showed that accumulation of a diversity of proteins overall, i.e. in eight out of nine assayed proteins, was associated with mRNA expression levels; however, posttranslational modifications were the likely explanation for decreased accumulation of one of the assayed proteins. Generally speaking, our analysis of differentially accumulated proteins in seedlings under cold stress elucidates the molecular mechanisms involved in cold tolerance in *A. aphylla* and other species.

Availability of data and material

The datasets supporting the conclusions of this article are available in the Gene Ontology (http://www.geneontology.org), Kyoto Encyclopedia of Genes and Genomes (http://www.genome.jp/kegg/ or http://www.kegg.jp/) and Uniprot (http://www.uniprot.org/).

Disclosure statement

No potential conflict of interest was reported by the authors.

References

Asada K. 1999. The water cycle in chloroplasts: scavenging of active oxygens and dissipation of excess photons. Annu Rev Plant Physiol Plant Mol Biol. 50:601–639. doi:10.1146/annurev.arplant.50.1.601.

Chen J. 2015. Study on differentially expressed proteome in response to low temperature in alfalfa [PhD thesis]. Harbin (China): Harbin Normal University.

Chen JH, Tian QQ, Pang T, Jiang LB, Wu RL, Xia XL, Yin WL. 2014. Deep-sequencing transcriptome analysis of low temperature perception in a desert tree, *Populus euphratica*. BMC Genomics. 15:326. doi:10.1186/1471-2164-15-326.

Cheng X, Deng G, Su Y, Liu JJ, Yang Y, Du GH, Chen ZY, Liu FH. 2016. Protein mechanisms in response to NaCl-stress of salt-tolerant and salt-sensitive industrial hemp based on iTRAQ technology. Ind Crop Prod. 83:444–452. doi:10.1016/j.indcrop.2015.12.086.

Cui SX, Huang F, Wang J, Ma X, Cheng YS, Liu JY. 2005. A proteomic analysis of cold stress responses in rice seedlings. Proteomics. 5:3162–3172. doi:10.1002/pmic.200401148.

Cyr DM, Langer T, Douglas MG. 1994. DnaJ-like proteins: molecular chaperones and specific regulators of Hsp70. Trends Biochem Sci. 19:176–181. doi:10.1016/0968-0004(94)90281-X.

Du CX, Fan HF, Guo SR, Tezuka T, Li J. 2010. Proteomic analysis of cucumber seedling roots subjected to salt stress. Phytochemistry. 71:1450–1459. doi:10.1016/j.phytochem.2010.05.020.

Foyer CH, Noctor G. 2000. Tansley review No. 112: oxygen processing in photosynthesis: regulation and signalling. New Phytol. 146:359–388. doi:10.1046/j.1469-8137.2000.00667.x.

Giovanni C, Maurizio B, Luca M, Laura S, Gian MG, Barbara C, Paola O, Luciano Z, Pier GR. 2004. Blue silver: a very sensitive colloidal Coomassie G-250 staining for proteome analysis. Electrophoresis. 25:1327–1333. doi:10.1002/elps.200305844.

Han JX, Wei Y, Yan C, An SZ. 2011. The vivipary characteristic of *Anabasis elatior* and its ecological adaptation. Acta Ecol Sin. 31:2662–2668.

Hasanuzzaman M, Hossain MA, Fujita M. 2012. Exogenous selenium pretreatment protects rapeseed seedlings from cadmium-induced oxidative stress by upregulating antioxidant defense and methylglyoxal detoxification systems. Biol Trace Elem Res. 149(2):248–261. doi:10.1007/s12011-012-9419-4.

Hu YH, Zhang QX, Wang KL, Zhang ZF. 2000. Ultrastructural changes of *Chrysanthemum* leaves exposed to low temperature. J Laiyang Agric Coll. 17:38–43.

Huang SW, Li RQ, Zhang ZH, Li L, Gu XF, Fan W, William L, Wang XW, Xie BY, Ni PX, et al. 2009. The genome of the cucumber, *Cucumis sativus L*. Nat Genet. 41:1275–1281. doi:10.1038/ng.475.

Huang AY, Wu ZL. 1999. Determination of glutathione peroxidase in rice seedlings. J Southwest Agric Univ. 21:1–4.

Isaacson T, Damasceno CM, Saravanan RS, He Y, Catalá C, Saladié M, Rose JK. 2006. Sample extraction techniques for enhanced proteomics analysis of plant tissues. Nat Protoc. 1:769–774. doi:10.1038/nprot.2006.102.

Janda T, Majlath I, Szalai G. 2014. Interaction of temperature and light in the development of freezing tolerance in plants. J Plant Growth Regul. 33:460–469. doi:10.1007/s00344-013-9381-1.

Jiang Y, Yang B, Harris NS, Deyholos MK. 2007. Comparative proteomic analysis of NaCl stress-responsive proteins in *Arabidopsis* roots. J Exp Bot. 58:3591–3607. doi:10.1093/jxb/erm207.

Kang JM. 2008. Study on the physiological and biochemical response and differentially expressed preteome under cold stress in Buffalograss [PhD thesis]. Beijing: Chinese Academy of Agricultural Sciences.

Ke JY, Ma HL, Gu X, Thelen A, Brunzelle JS, Li JY, Xu HE, Melcher K. 2015. Structural basis for recognition of diverse transcriptional repressors by the TOPLESS family of corepressors. Sci Adv. 1: e1500107. doi:10.1126/sciadv.1500107.

Kinoshita H, Nagasaki J, Yoshikawa N, Yamamoto A, Takito S, Kawasaki M, Sugiyama T, Miyake H, Weber APM, Taniguchi M. 2011. The chloroplastic 2-oxoglutarate/malate transporter has dual function as the malate valve and in carbon/nitrogen metabolism. Plant J. 65:15–26. doi:10.1111/j.1365-313X.2010.04397.x.

Krzysztof L, Agnieszka L, Szymon Z. 2008. Chaperones in control of protein disaggregation. Embo J. 27:328–335. doi:10.1038/sj.emboj. 7601970.

Lai QA, Hu JJ, Sun JR. 2001. Adenylate kinase and cellular apoptosis. Prog Biochem Biophys. 28:1–3.

Laura RU, Sarah MH, James MS, Thea W, Lindemanna W, Sengupta-Gopalana C, Zhang JF. 2011. Identification of salt responsive genes using comparative microarray analysis in upland cotton (*Gossypium hirsutum L.*). Plant Sci 180:461–469. doi:10.1016/j. plantsci.2010.10.009.

Li ZY, Long RC, Zhang TJ, Yang QC, Kang JM. 2016. Research progress on plant heat shock protein. Biotechnol Bull. 32:7–13.

Lu W, Tang XL, Huo YQ, Xu R, Qi SD, Huang JG, Zheng CC, Wu CA. 2012. Identification and characterization of fructose 1,6-bisphosphate

aldolase genes in *Arabidopsis* reveal a gene family with diverse responses to abiotic stresses. Gene. 503:65–74. doi:10.1016/j.gene. 2012.04.042.

Lukatkin AS. 2002. Contribution of oxidative stress to the development of cold-induced damage to leaves of chilling-sensitive plants: 2. The activity of antioxidant enzymes during plant chilling. Russ J Plant Physiol. 49:782–788. doi:10.1023/A:1020965629243.

Mazur BJ, Chui CF, Smith JK. 1987. Isolation and characterization of plant genes coding for acetolactate synthase, the target enzyme for two classes of herbicides. Physiol Plant. 85:1110–1117. doi:10.1104/ pp.85.4.1110.

Medina J, Bargues M, Terol J, Pérez-Alonso M, Salinas J. 1999. The *Arabidopsis* CBF gene family is composed of three genes encoding AP2 domain-containing proteins whose expression is accumulated by low temperature but not by abscisic acid or dehydration. Plant Physiol. 119:463–470.

Mirvat R, Francesco S, Stefano M. 2016. Role of ion transporters in salinity resistance in plants. Environ Control Biol. 54:1–6. doi:10.2525/ ecb.54.1.

Moreau M, Westlake T, Zampogna G, Popescu G, Tian M, Noutsos C, Popescu S. 2013. The *Arabidopsis* oligopeptidases TOP1 and TOP2 are salicylic acid targets that modulate SA-mediated signaling and the immune response. Plant J. 76:603–614. doi:10.1111/tpj.12320.

Nathalie D, Joel D, Nicole B. 1998. Molecular cloning and characterization of tomato cDNAs encoding glutathione peroxidase-like proteins. Eur J Biochem. 253:445–451. doi:10.1046/j.1432-1327.1998. 2530445.x.

Neilson KA, Mariani M, Haynes PA. 2011. Quantitative proteomic analysis of cold-responsive proteins in rice. Proteomics. 11:1696–1706. doi:10.1002/pmic.201000727.

Noctor G, Jouanin L, Foyer CH, Arisi ACM. 1999. Photorespiratory glycine enhances glutathione accumulation in both the chloroplastic and cytosolic compartments. J Exp Bot. 50:1157–1167. doi:10.1093/jxb/ 50.336.1157.

Nordin K, Vahala T, Palva ET. 1993. Differential expression of two related, low-temperature-induced genes in *Arabidopsis thaliana (L.) Heynh*. Plant Mol Biol. 21:641–653. doi:10.1007/BF00014547.

Palmieri MC, Lindermayr C, Bauwe H, Steinhauser C, Durner J. 2010. Regulation of plant glycine decarboxylase by s-nitrosylation and glutathionylation. Physiol Plant. 152:1514–1528. doi:10.1104/pp.109. 152579.

Pang SZ. 2015. Research on physiological indeces and differences in protein expression of banana seedling leaves under cold stress [master's thesis]. Nanning (China): Guangxi University.

Pendle AF, Clark GP, Boon R, Lewandowska D, Lam YW, Andersen J, Mann M, Lamond AI, Brown JWS, Shaw PJ. 2004. Proteomic analysis of the *Arabidopsis* nucleolus suggests novel nucleolar functions. Mol Cell Biol. 16:260–269. doi:10.1091/mbc.E04-09-0791.

Peng ZY, Wang MC, Li F, Lv HJ, Li CL, Xia GM. 2009. A proteomic study of the response to salinity and drought stress in an introgression strain of bread wheat. Mol Cell Proteomics. 8:2676–2686. doi:10. 1074/mcp.M900052-MCP200.

Picault N, Palmieri L, Pisano I, Hodges M, Palmieri F. 2002. Identification of a novel transporter for dicarboxylates and tricarboxylates in plant mitochondria. bacterial expression, reconstitution, functional characterization, and tissue distribution. J Biol Chem. 277:24204–24211. doi:10.1074/jbc.M202702200.

Ravanel S, Block MA, Rippert P, Jabrin S, Curien G, Rebeille F, Douce R. 2004. Methionine metabolism in plants: chloroplasts are autonomous for de novo methionine synthesis and can import S-adenosylmethionine from the cytosol. J Biol Chem. 279:22548–22557. doi:10.1074/ jbc.M313250200.

Reinbothe C, Pollmann S, Reinbothe S. 2010. Singlet oxygen signaling links photosynthesis to translation and plant growth. Plant Sci 15:499–506. doi:10.1016/j.tplants.2010.05.011.

Sánchez-Be P, Egea I, Sánchez-Ballesta MT, Martinez-Madrid C, Fernandez-Garcia N, Romojaro F, Olmos E, Estrella E, Bolarín M, Flores FB. 2012. Understanding the mechanisms of chilling injury in bell pepper fruits using the proteomic approach. J Proteomics. 75:5463–5478. doi:10.1016/j.jprot.2012.06.029.

Sasabe M, Soyano T, Takahashi Y, Sonobe S, Igarashi H, Itoh T, Hidaka M, Machida Y. 2006. Phosphorylation of NtMAP65-1 by a MAP kinase down-regulates its activity of microtubule bundling and stimulates progression of cytokinesis of tobacco cells. Genes Dev. 20:1004–1014. doi:10.1101/gad.1408106.

Shilov IV, Seymour SL, Patel AA, Loboda A, Tang W-H, Keating SP, Hunter CL, Nuwaysir LM, Schaeffer DA. 2007. The paragon algorithm, a next generation search engine that uses sequence temperature values and feature probabilities to identify peptides from tandem mass spectra. Mol Cell Proteomics. 6:1638–1655. doi:10.1074/mcp.T600050-MCP200.

Shimono Y, Kudo G. 2005. Comparisons of germination traits of alpine plants between fellfield and snowbed habitats. Ecol Res. 20:189–197. doi:10.1007/s11284-004-0031-8.

Smith PK, Krohn RI, Hermanson GT, Mallia AK, Gartner FH, Provenzano MD, Fujimoto EK, Goeke NM, Olson BJ, Klenk DC. 1985. Measurement of protein using bicinchoninic acid. Anal Biochem. 150:76–85. doi:10.1016/0003-2697(85)90442-7.

Sun ZL. 2011. Differently proteomics research on Chorispora bungeana under low temperature [PhD thesis]. Lanzhou (China): Lanzhou University.

Tan LL. 2012. Transcriptome analysis of cold tolerance mechanisms of Chorispora bungenan [PhD thesis]. Lanzhou (China): Lanzhou University.

Wang YJ. 2013. iTRAQ-based proteomics analysis of Lycium ruthenicum Murr. with salt (NaCl) treatment [master's thesis]. Lanzhou (China): Lanzhou University.

Wang XK, Huang JL. 2015. Principles and techniques of plant physiology and biochemistry experiment. Beijing: Higher Education Press.

Wang M, Li YY, Niu PX, Chu GM. 2015. Spatial pattern formation and intraspecific competition of Anabasis aphylla L. population in the diluvial fan of junggar basin, NM China. Pak J Bot. 47:543–550.

Wang XY, Shan XH, Wu Y, Su SZ, Li SP, Liu HK, Han JY, Xue CM, Yuan YP. 2016. iTRAQ-based quantitative proteomic analysis reveals new metabolic pathways responding to chilling stress in maize seedlings. J Proteomics. 146:14–24. doi:10.1016/j.jprot.2016.06.007.

Wang JG, Tan HZ, Li YH, Ma Y, Li ZM, Guddat LW. 2011. Chemical synthesis, in vitro acetohydroxyacid synthase (AHAS) inhibition, herbicidal activity, and computational studies of isatin derivatives. J Agri Food Chem. 59:9892–9900. doi:10.1021/jf2021607.

Wang WX, Vinocur B, Shoseyov O, Altman A. 2004. Role of plant heat-shock proteins and molecular chaperones in the abiotic stress response. Trends Plant Sci. 9:244–252. doi:10.1016/j.tplants.2004.03.006.

Wang Y, Zhang WZ, Song LF, Zou JJ, Su Z, Wu WH. 2008. Transcriptome analyses show changes in gene expression to accompany pollen germination and tube growth in Arabidopsis. Physiol Plant. 148:1201–1211. doi:10.1104/pp.108.126375.

Wei BY, Zhang JZ, Pang CX, Yu H, Guo DS, Jiang H, Ding MX, Chen ZY, Tao Q, Gu HY, et al. 2015. The molecular mechanism of sporocyteless/nozzle in controlling Arabidopsis ovule development. Cell Res. 25:121–134. doi:10.1038/cr.2014.145.

Welin BV, Olson A, Palva ET. 1995. Structure and organization of two closely related low-temperature-induced dhn/lea/rab-like genes in Arabidopsis thaliana (L.)heynh. Plant Mol Biol. 29:391–395. doi:10.1007/BF00043662.

Witzel K, Weidner A, Surabhi GK, Börner A, Mock HP. 2009. Salt stress-induced alterations in the root proteome of barley genotypes with contrasting response towards salinity. J Exp Bot. 60:3545–3557. doi:10.1093/jxb/erp198.

Xie H, Yang DH, Yao H, Bai G, Zhang YH, Xiao BG. 2016. iTRAQ-based quantitative proteomic analysis reveals proteomic changes in leaves of cultivated tobacco (Nicotiana tabacum) in response to drought stress. Biochem Biophys Res Commun. 469:768–775. doi:10.1016/j.bbrc.2015.11.133.

Xu N. 2007. Effect of cold stress on physiological metabolism of Buxus sempervirens [PhD thesis]. Harbin (China): Northeast Forestry University.

Xu C, Sibicky T, Huang B. 2010. Protein profile analysis of salt-responsive proteins in leaves and roots in two cultivars of creeping bentgrass differing in salinity tolerance. Plant Cell Rep. 29:595–615. doi:10.1007/s00299-010-0847-3.

Yan SP, Zhang QY, Tang ZC, Su WA, Sun WN. 2006. Comparative proteomic analysis provides new insights into chilling stress responses in rice. Mol Cell Proteomics. 5:484–496. doi:10.1074/mcp.M500251-MCP200.

Yang LT, Qi YP, Lu YB, Guo P, Sang W, Feng H, Zhang HX, Chen LS. 2013. iTRAQ protein profile analysis of Citrus sinensis roots in response to long-term boron-deficiency. J Proteomics. 93:197–206. doi:10.1016/j.jprot.2013.04.025.

Yue N, Zheng CX, Bai X, Hao JQ. 2009. Proteomics analysis of heteromorphic leaves of Populus euphratica Oliv. China Biotechnol. 29:40–44.

Zhao Q, Zhang H, Wang T, Chen SX, Dai SJ. 2013. Proteomics-based investigation of salt-responsive mechanisms in plant roots. J Proteomics. 82:230–253. doi:10.1016/j.jprot.2013.01.024.

Zhou P. 2013. Proteomic analysis of rice seedlings under cold stress [master's thesis]. Nanning (China): Guangxi University.

Zhou XY, Peng SY, Zhou SF, Fu FL, Yu HQ, Li WC. 2016. Evaluation of internal reference genes for quantitative real-time PCR in Ammopiptanthusnanus. Nanning (China): Guihaia.

Zhu GL. 1990. Plant physiology experiments. Beijing: Peking University Press.